Mater. Res. Soc. Symp. Proc. Vol. 1295 © 2011 Materials Research Society
DOI: 10.1557/opl.2011.350

Microfracture Test of $Mg_{12}ZnY$ Intermetallic Compound in Mg-Zn-Y Alloys

Hajime Yoshimura, Shun Matsuyama, Mitsuhiro Matsuda, Masaaki Otsu, Kazuki Takashima, Yoshihito Kawamura
Department of Materials Science and Engineering, Kumamoto University, 2-39-1, Kurokami, Kumamoto, Japan

ABSTRACT

A Mg-Zn-Y alloy including a $Mg_{12}ZnY$ intermetallic compound exhibits excellent mechanical properties as compared to conventional magnesium alloys. The superior mechanical properties of this alloy seem to originate from the $Mg_{12}ZnY$ intermetallic compound; however, the mechanical properties of $Mg_{12}ZnY$ itself have not yet been fully investigated owing to the small size of this compound. In this study, a microfracture test was performed to investigate the fracture properties of the $Mg_{12}ZnY$ intermetallic compound. The material used in this test was a $Mg_{88}Zn_5Y_7$ alloy. Micro-sized cantilever specimens composed of $Mg_{12}ZnY$, with dimensions of $10 \times 20 \times 50$ μm^3, were prepared selectively isolated from the $Mg_{88}Zn_5Y_7$ alloy using focused ion beam (FIB) machining. Notches with a width of 0.5 μm and a depth of 5 μm were also introduced into the micro-sized specimens. Microfracture tests were performed using a mechanical testing machine for microscale materials. The fracture toughness values (K_Q) of $Mg_{12}ZnY$ were 1.2−3.0 MPam$^{1/2}$. TEM observations indicated that the K_Q values were dependent on the crack orientation in $Mg_{12}ZnY$, with the higher K_Q values correlating with cracks propagating parallel to the c-axis of $Mg_{12}ZnY$. This suggests that the fracture toughness of Mg-Zn-Y alloys can be improved by controlling the orientation of the $Mg_{12}ZnY$ compound.

INTRODUCTION

From an environmental point of view, magnesium alloys such as AZ31 and ZK60 are attractive light-weight structural materials owing to their low density, high specific strength, good damping properties, and the fact that these materials can be easily recycled. Consequently, magnesium alloys are incorporated into a variety of applications, including automotive parts and aerospace and electronic applications [1, 2]. However, their low strength and poor ductility hinder their widespread application. Therefore, great effort has been expended in improving the strength and ductility of magnesium alloys. Recently, Kawamura *et al.* reported that Mg-Zn-Y alloys with a long-period stacking ordered (LPSO) phase exhibit higher strength, better ductility, and superior heat resistance as compared to conventional Mg alloys [3]. These excellent properties originate not only from α-Mg matrix grain refinement but also from a novel precipitate with a LPSO phase [3]. The LPSO phase consists of a periodical stacking of close-packed planes, which correspond to (0001) in hcp. In a related study, Abe *et al.* reported a peculiar chemical order of Y and Zn atoms in Mg-based LPSO planes, that is, the periodical enrichment of Y and Zn atoms at particular close-packed planes [4]. Padezhnova *et al.* investigated the Mg-Zn-Y ternary phase diagram around the Mg corner and found a stable LPSO

phase with a composition of $Mg_{12}ZnY$, which is referred to as the X-phase [5]. Hagihara *et al.* reported that the $Mg_{12}ZnY$ intermetallic compound exhibits plastic deformation with kinking [6].

In order to apply such bi-modal alloys including Mg-Zn-Y alloys, it is important to investigate the fracture properties and the fracture behavior of its constituent phases. However, because the sizes of its constituent phases are in the order of micrometers, the present macroscale fracture tests cannot be applied for the measurement of fracture toughness and the investigation of the fracture behavior of each constituent phase. We have developed a microscale testing machine; this machine can be used to measure the tensile and bending properties as well as the fracture toughness of specimens with dimensions of 10–50 μm [7]. Because the volume fraction of the $Mg_{12}ZnY$ intermetallic compound in the $Mg_{88}Zn_5Y_7$ alloy is approximately 90%, it is possible to prepare a micro-sized specimen composed primarily of the $Mg_{12}ZnY$ intermetallic compound. If this testing machine is applied, it is possible to investigate the fracture toughness and the fracture behavior of the $Mg_{12}ZnY$ intermetallic compound.

In this study, the fracture toughness and the fracture behavior of the $Mg_{12}ZnY$ intermetallic compound were investigated using a microscale testing machine.

EXPERIMENTAL PROCEDURE

A $Mg_{88}Zn_5Y_7$ alloy was used in this investigation. This material was hot extruded at 723 K, with an extrusion ratio of 10. Figures 1(a) and (b) show the scanning electron micrographs of the microstructure of this alloy.

Micro-sized specimens were cut, either orthogonal (Type-A) or parallel (Type-B) to the direction of extrusion, from the rods of the $Mg_{88}Zn_5Y_7$ alloy. The specimens were then polished on both sides to form foils with a thickness of approximately 20 μm. Micro-sized cantilever beam specimens were prepared by focused ion beam (FIB) machining. Figure 2 shows a scanning electron micrograph of a specimen on a microscale. The length (*L*), breadth (*B*), and thickness (*W*) of the specimens were 50, ~20, and 10 μm, respectively.

The loading position was located 40 μm away from the fixed end of the specimen as indicated by the arrow in Figure 2. Notches with a width of 0.5 μm and a depth of 3.5−5.0 μm were also introduced into the micro-sized specimens, 10 μm away from the fixed end of the specimen, using FIB machining. A microscale mechanical testing machine was used to test the fracture toughness of the microsized specimens. The load resolution of this testing machine was 20 μN, and its the displacement resolution was 0.2 nm. The loading position was adjusted using a precise X-Y stage, with a translation resolution of 0.05 μm.

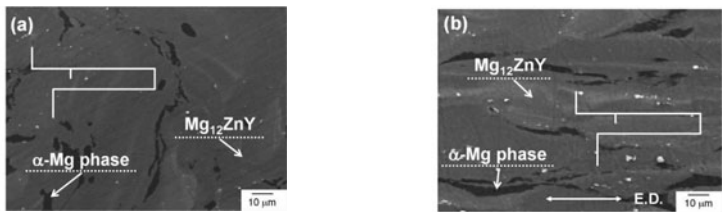

Figure 1. Scanning electron micrographs of the microstructure of $Mg_{88}Zn_5Y_7$ alloy. (a) Type-A specimen and (b) Type-B specimen

After the fracture tests were performed, the fracture surfaces were observed by scanning electron microscopy (SEM). A sample, to be analyzed via TEM, was isolated from the fractured specimen using FIB, and crack paths were observed.

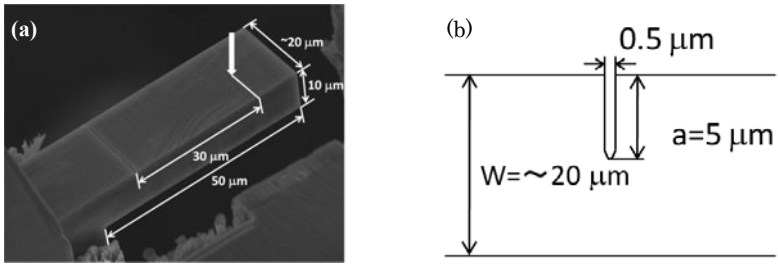

Figure 2. (a) Scanning electron micrograph of a micro-sized specimen prepared from $Mg_{88}Zn_5Y_7$ alloy and (b) notch geometry.

RESULTS AND DISCUSSION

The fracture toughness value of $Mg_{12}ZnY$ intermetallic compound

Figure 3 shows the load-displacement curves for the specimen obtained from the $Mg_{88}Zn_5Y_7$ alloys (hereafter referred to as the $Mg_{12}ZnY$ specimen). The difference in the maximum load is caused by the specimen size and notch length. Both Type-A and Type-B specimens of $Mg_{12}ZnY$ were fractured in a brittle manner. Therefore, it is assumed that the crack originates at and propagates from the maximum load.

The fracture toughness values (K_Q) were calculated from the maximum load using the following equations for stress intensity (K) for a notched cantilever beam [8].

$$K = \frac{6P_Q S}{W^2 B}\sqrt{\pi a}F(a/W), \tag{1}$$

where

$$F(a/W) = 1.122 - 1.40 - 1.40(a/W) + 7.33(a/W)^2 - 13.08(a/W)^3 + 14.0(a/W)^4 \tag{2}$$

In equation (1), a, P_Q, and S are the total crack length, the failure load, and the distance between the loading point and the notch position, respectively. The maximum failure load (P_Q) was considered to be the maximum load of the load-displacement curve. After the fracture tests were performed, a was measured from the fracture surface using scanning electron micrographs.

Because the K_Q values do not satisfy the microscale conditions of this study, provisional K_Q values were considered. The calculated fracture toughness values for both types of $Mg_{12}ZnY$ specimens are shown in Figure 4. The fracture toughness values of Type-A and Type-B specimens were determined to be 1.2−1.3 $MPam^{1/2}$ and 1.4−3.0 $MPam^{1/2}$, respectively. The K_Q value of the Type-B $Mg_{12}ZnY$ specimen, which was cut parallel to the extrusion direction of the

$Mg_{88}Zn_5Y_7$ alloy, was higher than that of the Type-A $Mg_{12}ZnY$ specimen.

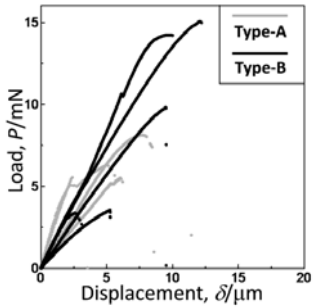

Figure 3. Load-displacement curves obtained during fracture toughness testing of $Mg_{88}Zn_5Y_7$ alloy.

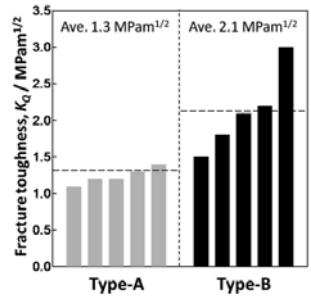

Figure 4. Fracture toughness values obtained by fracture testing of $Mg_{88}Zn_5Y_7$ alloy.

Fracture behavior of $Mg_{12}ZnY$ intermetallic compound

Figures 5(a) and (b) show a scanning electron micrograph of the fracture surface after the fracture tests. The fracture surface of the Type-A $Mg_{12}ZnY$ specimen had cleavage-like facets (Figure 5(a)), whereas the fracture surface of the Type-B $Mg_{12}ZnY$ specimen had many asperities (Figure 5(b)). Figure 5 shows that the fracture behavior of the Type-A $Mg_{12}ZnY$ intermetallic compound is different from that of the Type-B specimen. These results show that the $Mg_{12}ZnY$ intermetallic compound exhibits anisotropy. This material has strong a basal plane texture owing to the extrusion process [9]. Therefore, a TEM sample was prepared from the center part of the fractured specimen by FIB to determine the crystal orientation of the $Mg_{12}ZnY$ intermetallic compound.

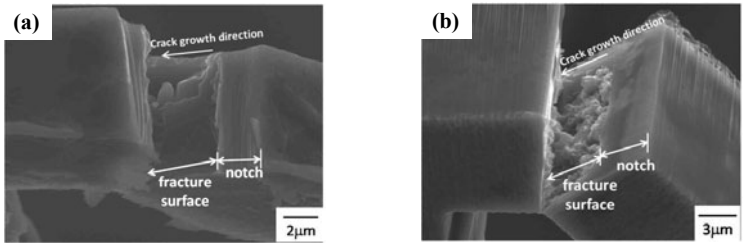

Figure 5. Scanning electron micrographs of the $Mg_{12}ZnY$ specimens after fracture testing. (a) Type-A specimen and (b) Type-B specimen.

The crack path of the Type-A $Mg_{12}ZnY$ specimen (K_Q = 1.3 $MPam^{1/2}$) was observed by TEM (Figure 6). The crack propagated linearly when the c-axis was perpendicular to the crack

growth direction, as shown in Figure 6(a). Conversely, Figure 6(b) shows that, when the c-axis is parallel to the crack growth direction, the crack bends. The crack path of the Type-B $Mg_{12}ZnY$ specimen (K_Q = 3.0 $MPam^{1/2}$) was also determined via TEM (Figure 7). In Figure 7, the black and white areas that follow the crack path represent the deposition layer and the amorphous layer, respectively, when the TEM sample was prepared by FIB. Figures 7(a) and (b) show that the crack propagated parallel to the c-axis. Thus, we can conclude that the fracture toughness is higher when the crack propagates parallel to the c-axis than when it propagates perpendicular to the c-axis.

These results show that the fracture properties of the Mg-Zn-Y alloy can be improved by controlling the orientation of the $Mg_{12}ZnY$ intermetallic compound.

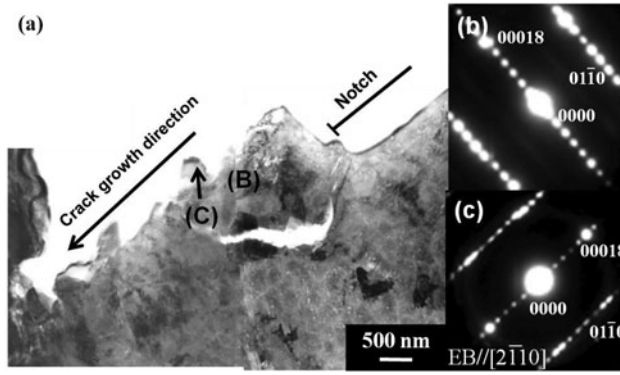

Figure 6. (a) Bright field image of Type-A $Mg_{12}ZnY$ specimen alloy and (b) and (c) electron diffraction patterns selected by (B) and (C) in image.

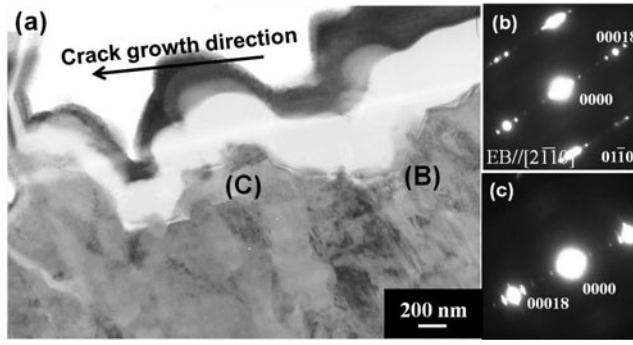

Figure 7. (a) Bright field image of Type-B $Mg_{12}ZnY$ specimen alloy and (b) and (c) electron diffraction patterns selected by (B) and (C) in image.

CONCLUSIONS

A micro-sized testing technique was used for the investigation of the fracture properties of $Mg_{12}ZnY$ intermetallic compound specimens. The following conclusions were obtained:

(1) Fractures occurred in a brittle manner, and anisotropy in the fracture toughness was observed,

(2) The crack tended to propagate along the (0001) plane, and crack initiation and growth resistance to the [0001] direction were higher, which is the reason for anisotropy in fracture toughness,

(3) The fracture properties of Mg-Zn-Y alloys can be improved by controlling the orientation of $Mg_{12}ZnY$.

REFERENCES

1. H. Somekawa and T. Mukai, *Scr. Mater.* **53**, 541 (2005).
2. H. Somekawa, A. Singh and T. Mukai, *J. Mater. Res*. **22**, 965 (2007).
3. S. Yoshimoto, M. Yamasaki and Y. Kawamura, *Mater. Trans.* **47**, 959 (2006).
4. E. Abe, Y. Kawamura, K. Hayashi and A. Inoue, *Acta Mater.* **50**, 3845 (2002).
5. E. M. Padezhnova, E. V. Melnik, R. A. Miliyevskiy, T. V. Dobatkina and V. V. Kinzhibalo, *Russ. Metall. (Metally) (Engl. Transl.)* **4**, 185 (1982).
6. K. Hagihara, N. Yokotani and Y. Umekoshi, *Intermetallics* **18**, 267 (2010).
7. K. Takashima and Y. Higo, *Fatig. Fract. Eng. Mater. Str.* **28**, 703(2005).
8. H. Okamura, *Introduction to Linear Fracture Mechanics*, (Baifukan, Tokyo, 1976), p. 218 (in Japanese).
9. T. Yamaguchi, K. Saito and Y. Kawamura, *J. JILM* **57**, 571 (2007).